

Long wavelength InGaAsP/InP distributed feedback lasers grown by chemical beam epitaxy

W.T. Tsang^a, F.S. Choa^{b,1}, M.C. Wu^a, Y.K. Chen^a, R.A. Logan^a, S.N.G. Chu^a,
A.M. Sergent^a, P. Magill^b, K.C. Reichmann^b and C.A. Burrus^b

^a AT&AT Bell Laboratories, Murray Hill, New Jersey 07974, USA

^b AT&AT Bell Laboratories, Crawford Hill, Holmdel, New Jersey 07733, USA

We have demonstrated successful operation of long wavelength InGaAsP low threshold-current gain-coupled DFB lasers. This is accomplished by using a InGaAsP quaternary grating or quantum well grating that absorbs the DFB emission. The use of a quantum well grating, in particular, greatly facilitates the reproducible regrowth (defect-free) over grating and the control of the coupling coefficient. CW threshold currents were in the range of 10–15 mA for 250 μm and 13–18 mA for 250 and 500 μm cavities, respectively. Slope efficiencies were high, ~ 0.4 mW/mA (both facets). SMSR was as high as 52 dB and remained in the same DFB mode with SMSR staying ~ 50 dB throughout the entire current range. Linewidth \times power products of 1.9–4.0 were measured with minimum linewidths of 1.8–2.2 MHz. No detectable chirp was measured under 2.5 Gb/s modulation. Unlike index-coupled DFB lasers in which mode partition events decrease slowly even when biased above threshold, these lasers have mode partition events shut off sharply as bias approaches threshold ($\geq 0.95 I_{\text{th}}$). A very small dispersion penalty of 1.0 dB was measured at 10^{-11} BER in transmission experiments using these lasers as sources at 1.7 Gb/s over an amplified fiber system of 239 km. No self-pulsation was observed in these gain-coupled DFB lasers.

1. Introduction

The oscillation wavelength degeneracy at the edges of the Bragg reflection band is a major problem in index-coupled DFB [1–5] lasers. One solution to this problem is the use of anti-reflection/high-reflection (AR/HR)-coated facets. This, however, causes a yield problem associated with the uncertainty of the facet phases [1]. Another solution is the incorporation of a $\lambda/4$ or corrugation-pitch modulated phase shift [2,3,6]. For perfect AR coatings, these lasers show a high yield, while deteriorating rapidly for reflectivities only a few percent [2]. Other drawbacks include that half of the power practically being wasted from the back facet and the high spatial hole burning caused by the $\lambda/4$ phase shift [3] (this is reduced by the corrugation-pitch modulation scheme [6]). The high spatial hole burning gives

rise to optical nonlinearity in the light-current ($L-I$) curves, increased spectral linewidth, and a less flat frequency-modulation response.

An alternative approach is the introduction of gain coupling [5,7,8]. Purely gain-coupled lasers theoretically should have one lasing mode exactly at the Bragg wavelength for AR-coated facets, thereby solving the degeneracy problem [5]. It is shown theoretically [9,10] that even a small degree of gain coupling enhances the performance considerably in terms of threshold gain difference (side-mode-suppression ratio) and removes the degeneracy of an AR-coated DFB laser. Moreover, a complete elimination of spatial hole burning is possible [10]. This in turn will further increase the laser yield. For non-AR-coated lasers, it is shown [11,12] that there is a relevant improvement in yield even for a small amount of gain coupling. In addition, results also show a potential for lower feedback sensitivity compared to other DFB lasers [13]. The validity of the gain-coupled approach for semiconductor DFB

¹ Present address: University of Maryland, Baltimore, Maryland, USA.

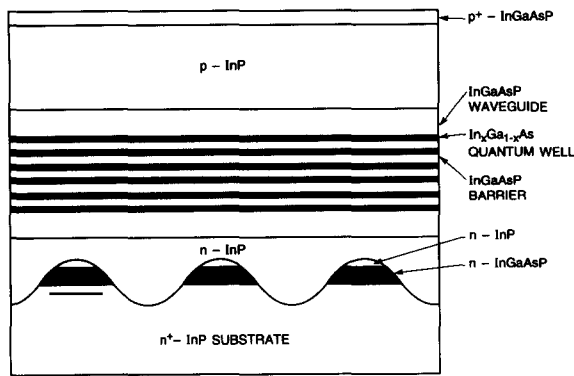


Fig. 1. Schematic diagram of the MQW DFB laser structure with a bottom buried loss-coupled quaternary grating.

lasers has been demonstrated recently in GaAs/AlGaAs lasers [7,8]. Very recently, 1.5 μm gain-coupled DFB lasers were also demonstrated using varying active layer thickness [14] and in AlGaInAs systems [15]. In this experiment, we demonstrate the use of loss-coupled (since the resultant effect is a periodic gain modulation, we will refer in the following as gain-coupled in accordance with the convention) InGaAsP quaternary grating and InGaAs/InP quantum well grating for long wavelength DFB lasers. The amount of gain-coupling coefficient κ_g is controlled by the composition (bandgap) or thickness of the quaternary or InGaAs quantum well grating chosen.

2. Gain-coupled DFB lasers with quaternary grating

In fig. 1, we show schematically the proposed DFB laser structure. As an illustrative example, a 1.5 μm InGaAs/InGaAsP with a InGaAsP quaternary grating is shown. The grating grooves have etched through the InGaAsP layer to form isolated InGaAsP grating lines buried in InP. This yields the largest possible gain modulation since the burying InP is lossless. To fabricate this, a uniform layer of 20 nm n-type InGaAsP (bandgap wavelength $\lambda = 1.56 \mu\text{m}$, for convenience, it will be referred to as $Q_{1.56}$) was grown on a 2 inch diameter (100)-oriented n-InP substrate capped

by a 5 nm InP top layer. This ensures that there is optical absorption at the lasing wavelength, 1.55 μm . It has been shown previously that the present CBE system is capable of producing layers having a thickness uniformity of $\leq \pm 1.0\%$ and a photoluminescence (PL) peak wavelength uniformity of $\leq \pm 5 \text{ nm}$ (as good as $\equiv 1.5 \text{ nm}$) [16,17]. Recent results from other research groups also obtained thickness variations $\leq 0.75\%$ and bandgap wavelength variations of InGaAsP quaternaries $\leq \pm 1 \text{ nm}$ over 3 inch diameter wafers with CBE [18]. First order gratings were prepared by standard holographic techniques and wet etching, and had an amplitude of $\sim 50 \text{ nm}$. No precise grating depth control was exercised here as long as the QWs were completely etched through. After cleaning, the sample was re-introduced into the CBE system for MQW laser regrowth. An n-type InP spacer layer of the desired thickness (65 nm in the present laser) was grown. The thickness of this layer will also affect the value of both the index- and the gain-coupled coefficients. Because the $Q_{1.56}$ is thin and the top surface is capped with InP layers, subsequent regrowth of InP over such a grating is essentially the same as growing InP on InP. This makes regrowth over grating a trivial task and guarantees defect-free as examined by TEM. This was then followed by the standard strained-layer 6-QW separate confinement heterostructure (SCH) [19,20]. The quaternary, $Q_{1.25}$, waveguide layers were 52.2 nm each. The strained-layer $\text{In}_{0.6}\text{Ga}_{0.4}\text{As}$ QWs and $Q_{1.25}$ barriers were 5 and 18.6 nm, respectively. These laser wafers were further processed into buried heterostructure employing MOVPE regrowth of Fe-doped InP at 630°C.

In fig. 2, we show the photoluminescence (PL) spectrum if the grating $Q_{1.56}$ measured before grating-etching together with the PL spectrum from the 6-QW $\text{In}_{0.6}\text{Ga}_{0.4}\text{As}$ (5 nm)/ $Q_{1.25}$ (18.6 nm) active-layer DFB laser wafer after regrowth over the $Q_{1.56}$ grating. It is seen that optical absorption has extended well beyond 1550 nm. This suggests that the present $Q_{1.56}$ grating will produce a gain-coupled component in addition to the index-coupled component due to index refraction difference between InP and $Q_{1.56}$. It is important to point out that this index refraction

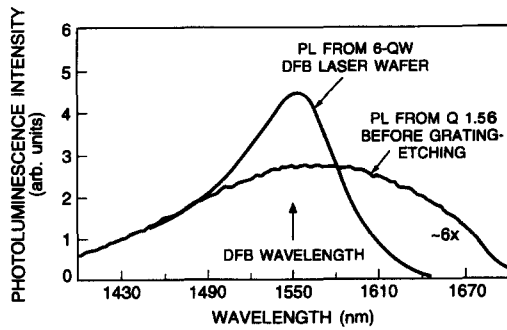


Fig. 2. Photoluminescence spectra from the grating $Q_{1.56}$ measured before grating-etching and the 6-QW $\text{In}_{0.6}\text{Ga}_{0.4}\text{As}/Q_{1.25}$ active-layer DFB laser wafer after regrowth over the $Q_{1.56}$ grating.

difference increases as the quaternary bandgap decreases. Thus, thinner quaternary layer is needed for the same index refraction difference. This facilitates the regrowth over the grating.

The resulting DFB lasers (250 μm long cavity and both facets as-cleaved) operated at 1.55 μm with CW threshold currents 10–15 mA and slope efficiencies up to 0.4 mW/mA (both facets). Such performance is similar to that of the index-coupled DFB lasers [21]. This indicates that with optimally designed gain-coupled DFB lasers, the presence of the loss-coupled grating did not noticeably increase the threshold currents and decrease the slope efficiencies. Side-mode suppression ratios (SMSR) as high as 52 dB have been obtained in as-cleaved lasers without facet coatings. In fact, these performance values are among the best DFB lasers. A typical light-current characteristic is shown in fig. 3. The inset shows the spectrum obtained at output power of ~ 20 mW/facet. A very large SMSR of 52 dB was obtained. The laser operated in the same DFB mode with SMSR above 45 dB starting above threshold and stayed at ~ 50 dB throughout the entire current range as shown in fig. 4. No mode jumps were observed in the threshold crossing in comparison with a similar structure but with purely index-coupled DFB lasers [21]. It is important to point out that the seven lasers CW-bonded for checking the spectra, all have the same single DFB mode (the longer wavelength one).

Since the $Q_{1.56}$ grating segments have higher

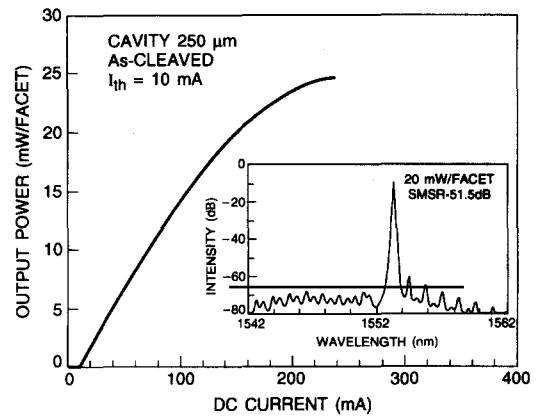


Fig. 3. Light-current characteristic of a typical as-cleaved CBE-grown buried heterostructure gain-coupled MQW DFB laser. The inset shows the spectrum obtained at an output power of ~ 20 mW/facet. A SMSR of 52 dB was measured.

refractive index and are optically absorbing, the Bragg mode, which has its standing-wave peaks aligned with these $Q_{1.56}$ segments will suffer more loss and has a shorter wavelength than the other Bragg mode which aligns with the InP troughs of the grating. This explanation is consistent with our experimental observation. Although this result is rather preliminary, it appears to agree with the theoretical expectation that even a small degree of gain coupling enhances the performance considerably in terms of threshold gain difference, and removes the degeneracy. Our estimated κ_g is ~ 4 cm^{-1} using an absorption loss of $\sim 2 \times 10^4$ cm^{-1} for $Q_{1.56}$. The κ_i is less than ≤ 50 cm^{-1} . No self-pulsation was observed.

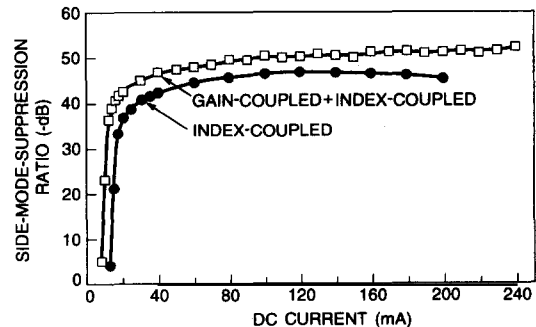


Fig. 4. SMSR as a function of injection current for a 1.5 μm wavelength gain-coupled and an index-coupled DFB laser.

3. Gain-coupled DFB lasers with quantum well gratings

To investigate gain-coupled DFB laser and achieve fine control of κ , we further propose a new grating layer structure using quantum wells. In fig. 5 we show schematically the proposed DFB laser structure. As an illustrative example, a $1.5 \mu\text{m}$ $\text{In}_x\text{Ga}_{1-x}\text{As}/\text{InGaAsP}$ multi-quantum well (MQW) active-layer laser with a 2-QW $\text{In}_y\text{Ga}_{1-y}\text{As}/\text{InP}$ grating is shown. The key innovation in this structure is the use of QW structure for the grating. This offers great design flexibility and several important advantages. (1) Because the QWs are thin and inter-leaved with InP barriers, and the top surface is capped with InP layer, subsequent regrowth of InP over such a grating is essentially the same as growing InP on InP. This makes regrowth over grating a trivial task and guarantees defect-free. (2) The coupling coefficient κ can be conveniently controlled by the number, the composition, or the thickness of the QWs. Further, the depth profile of the grating can be tailored by having QWs of different thicknesses or compositions or barriers. (3) Since the optimal coupling constant κL , where L is the laser cavity, should be approximately 1 to 2 for the best device performance [22], relatively weak grating effect is sufficient. Thus, in practice, only

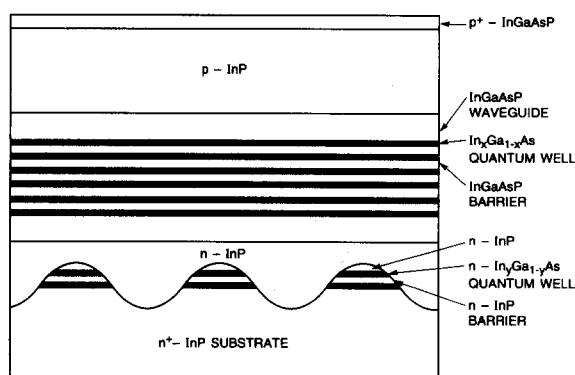


Fig. 5. Schematic drawing of the proposed DFB laser structure with quantum well (or superlattice) grating for optical feedback. As an illustrative example, a $1.5 \mu\text{m}$ $\text{In}_x\text{Ga}_{1-x}\text{As}/\text{InGaAsP}/\text{InP}$ 6-QW active-layer laser with a 2-QW $\text{In}_y\text{Ga}_{1-y}\text{As}$ grating is shown. Other design combinations can be used as discussed in the text.

very few Qws are needed. This allows all the QWs to be completely etched through during the grating formation (see, the example in fig. 1). As a result, the actual grating depth plays no role in affecting the κ . This significantly lessens the stringent requirement in grating depth control in conventional DFB laser structures. (4) Since the index of refraction of InGaAsP quaternary material increases as the bandgap of the material becomes narrower, by using narrower bandgap material for the grating quantum wells, the QW thickness can be further reduced. Furthermore, because of the quantum-size effect, the absorption edge of the QW grating can be designed to be above the lasing wavelength even if the same material composition as the active layer is used in the grating QWs. (5) On the other hand, if gain-(loss)-coupled grating is desired, the thickness or composition of grating QWs can be designed so that its absorption edge is below the lasing wavelength. Since the grating Qws can be made very thin, it may be possible to make the gain-coupling effect dominate over the index-coupling effect. If necessary, the grating Qws can have composition with narrower bulk bandgap than the active QW material. Fig. 5 illustrates such possibilities with $\text{In}_x\text{Ga}_{1-x}\text{As}/\text{InGaAsP}$ active QWs and $\text{In}_y\text{Ga}_{1-y}\text{As}/\text{InP}$ QW grating. In this example, x and y can be designed independently and varied over wide ranges. (6) The QW grating can also be composed of strained-layer, either tensile or compressive. This may further modify the coupling coefficient of TE and TM modes of the DFB lasers. (7) If desired, superlattice can be used in the grating instead of QWs. (8) Such QW grating can also be located on top of the active layers.

Therefore, it is seen that the introduction of QW (or superlattice) grating in DFB (or DBR) lasers will greatly facilitate the reproducible regrowth over grating and the control of the coupling coefficient. It will also provide a very convenient and effective scheme of achieving gain-coupled DFB lasers.

Fig. 6 shows a transmission electron microscope photograph (the cross-sectional view) of a 6-QW active-layer DFB laser with a 2-QW grating. The fuzzy outline of the InP/InP grating interface is due to non-exact perpendicular orien-

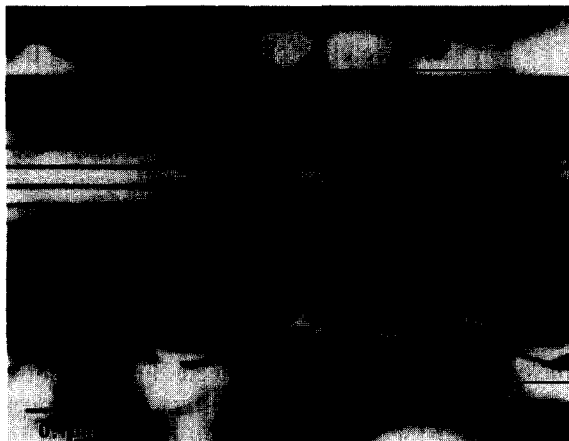


Fig. 6. TEM photograph of the cross-sectional view of a 6-QW $\text{In}_{0.6}\text{Ga}_{0.4}\text{As}$ (5 nm)/ $\text{Q}_{1.25}$ (18.6 nm) active-layer DFB laser with a 2-QW $\text{In}_{0.62}\text{Ga}_{0.38}\text{As}$ (4 nm)/InP (9.3 nm) grating.

tation of the sample with respect to the incident electron beam during viewing and the round uneven etched grating surface. Nevertheless, it is seen that the regrowth is defect-free. It is also seen that the InP spacer layer smooths out the surface corrugation quickly compared with growth of quaternary over InP gratings.

To fabricate this, a uniform stack of n-type InGaAs/InP QW (or superlattice) of the desired number, composition, and thickness having a thin InP cap layer for grating fabrication was grown first over a 2 inch diameter (100)-oriented n-InP substrate. We have fabricated such DFB laser wafers with the number of grating QWs varied from one to eight. For wafers with a large number of QWs, thinner QWs and InP barriers were used in order to maintain the total thickness ≤ 50 nm. In these cases, they behave more as superlattices than independent QW gratings. In the example shown by the TEM photograph in fig. 6, two $\text{In}_{0.62}\text{Ga}_{0.35}\text{As}$ (slightly In-richer than the $\text{In}_{0.6}\text{Ga}_{0.4}\text{As}$ active QWs) QWs of 4 nm and InP barrier of 9.3 nm were grown. The top InP cap layer was 9.3 nm. First order gratings were prepared by standard holographic techniques and wet etching and had an amplitude of ~ 48 nm as shown in fig. 6. No precise grating depth control was exercised here as long as the QWs were completely etched through. After cleaning, the

sample was re-introduced into the CBE system for MQW laser regrowth at a temperature of $\sim 540^\circ\text{C}$. Under such low temperature conditions, no grating erosion was ever observed. The detailed shape of the grating was well preserved as shown by the TEM photograph. An n-type InP spacer layer of the desired thickness (65 nm in the present laser) was grown. The thickness of this layer will also affect the value of κ . This was then followed by the standard strained-layer 6-QW separate confinement heterostructure (SCH). The quaternary, $\text{Q}_{1.25}$, waveguide layers were 52.2 nm each. The $\text{In}_{0.6}\text{Ga}_{0.4}\text{As}$ QWs and $\text{Q}_{1.25}$ barriers were 5 nm and 18.6 nm, respectively. These laser wafers were further processed into buried heterostructure employing MO-VPE regrowth of Fe-doped InP at 630°C .

We have studied the device performance of DFB lasers with various QW grating designs. Here, we will report the results obtained from a wafer with 2-QW $\text{In}_{0.62}\text{Ga}_{0.38}\text{As}$ grating (sample shown in fig. 6). In this particular wafer, because the gain peak is located sufficiently (38 nm) longer in wavelength (see fig. 7) than the DFB peak designated at 1550 nm, anti-reflection (AR) facet coatings ($\sim 5\%$ on both facets) were employed to push the gain-peak towards the shorter wavelength. When the gain-peak was located closer to the DFB peak in the other wafers, even as-cleaved lasers show high side-mode-suppression ratios

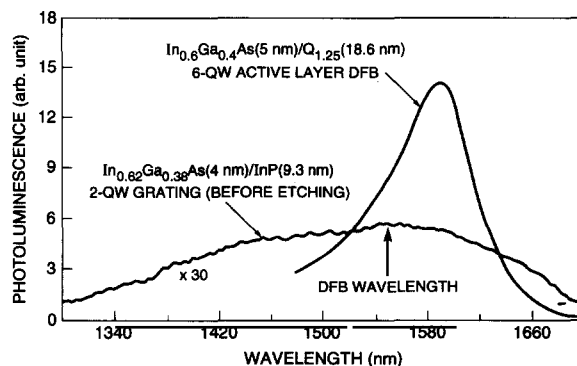


Fig. 7. Photoluminescence spectra from the two grating QWs before grating-etching, and from the 6-QW active-layer DFB laser wafer after regrowth over the grating. The optical absorption by the 2-QW grating has extended well beyond the intended DFB lasing wavelength at $1.55 \mu\text{m}$.

(SMSR). However, we choose to present the results from this particular wafer because the total thickness of the two QWs was only 8 nm and they were of $\text{In}_{0.62}\text{Ga}_{0.38}\text{As}$ material. This combination serves well to demonstrate the present proposed idea. The photoluminescence (PL) spectrum of this grating QWs was measured before grating etching and is shown in fig. 7 together with the PL spectrum from the 6-QW $\text{In}_{0.6}\text{Ga}_{0.4}\text{As}$ (5 nm)/ $\text{Q}_{1.25}$ (18.6 nm) active-layer DFB laser wafer after regrowth over the 2-QW grating. It is seen that optical absorption has extended well beyond 1550 nm. This suggests that the present QW grating will also produce a significant gain-(loss)-coupled component.

In fig. 8 we show the L - I characteristic of a typical 500 μm long laser. Output power of 46 mW/facet was obtained with a slope efficiency of ~ 0.2 mW/mA/facet. The inset shows the lasing spectrum at ~ 30 mW output. A SMSR of 47 dB was obtained. It is important to point out that even through the $\text{In}_{0.62}\text{Ga}_{0.38}\text{As}$ QW grating may introduce some additional loss, we have not observed unacceptable increase in threshold currents. For example, in the present case, the CW threshold currents were 13–18 mA even when the cavity length was 500 μm and both facets AR coated with the DFB mode far away from the gain peak. Fig. 9 shows the SMSR as a function of injection current. A SMSR of ~ 45 dB was

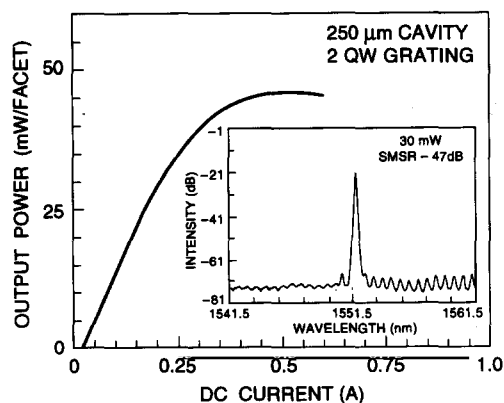


Fig. 8. Light-current characteristic of a typical 500 μm long laser with both facets AR-coated ($\sim 5\%$). The inset shows the lasing spectrum at ~ 30 mW.

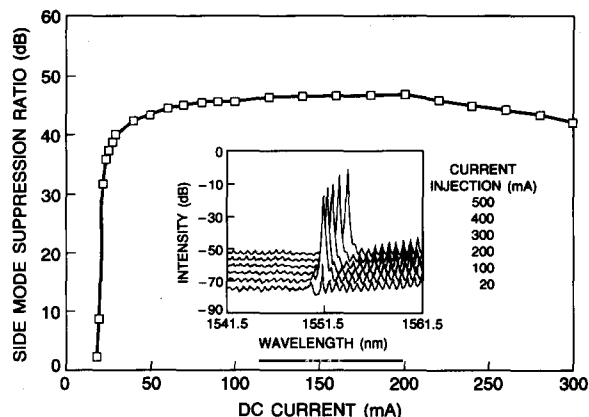


Fig. 9. SMSR as a function of injection current. The inset shows the spectra at different injection currents. Near threshold the DFB mode is relatively well centered with a small Bragg stop-band.

maintained throughout the entire current range once lasing started. The inset shows the actual spectra up to 500 mA. Near threshold the DFB mode is relatively well centered with a small Bragg stop-band. This indicates that the κ is small and there is the presence of gain-coupled component.

The linewidth of 250 μm and uncoated lasers were also measured as a function of output power. Linewidth \times power products of 1.9 to 4.0 were measured with minimum linewidths of 1.8–2.2 MHz. Under 2.5 Gb/s modulation (32 mA), no detectable chirp was measured on the optical spectrum analyzer which has a resolution of 0.1 nm. Mode partition characteristics at 2.5 Gb/s were measured with DC biased at $0.8I_{\text{th}}$, $0.9I_{\text{th}}$ and $1.0I_{\text{th}}$. It is found that mode partition events shut off sharply as bias approaches I_{th} ($\geq 0.95I_{\text{th}}$). Such behavior is very different from index-coupled DFB lasers in which the mode partition events decrease slowly even when biased above threshold. Transmission experiments were carried out using such lasers as sources at .17 Gb/s over an amplified fiber system of 239 km. A very small dispersion penalty of 1.0 dB was measured at 10^{-11} BER. Such small dispersion penalties are among the lowest observed with DBR lasers and index-coupled DFB lasers. We would like to emphasize here that the above laser performance

clearly demonstrates that these gain-coupled lasers are free of self-pulsation.

4. Summary

In summary, we have demonstrated successful operation of long wavelength InGaAsP low threshold-current gain-coupled DFB lasers. This is accomplished by using a InGaAsP quaternary grating or quantum well grating that absorbs the DFB emission. The use of a quantum well grating, in particular, greatly facilitates the reproducible regrowth (defect-free) over grating and the control of the coupling coefficient. CW threshold currents were in the range of 10–15 mA for 250 μm and 13–18 mA for 250 μm and 500 μm cavities, respectively. Slope efficiencies were high, ~ 0.4 mW/mA (both facets). SMSR was as high as 52 dB and remained in the same DFB mode with SMSR staying ~ 50 dB throughout the entire current range. Linewidth \times power products of 1.9–4.0 were measured with minimum linewidth of 1.8–2.2 MHz. No detectable chirp was measured under 2.5 Gb/s modulation. Unlike index-coupled DFB lasers in which mode partition events decrease slowly even when biased above threshold, these lasers have mode partition events shut off sharply as bias approaches threshold ($\geq 0.95I_{\text{th}}$). A very small dispersion penalty of 1.0 dB was measured at 10^{-11} BER in transmission experiments using these lasers as sources at 1.7 Gb/s over an amplified fiber system of 239 km. No self-pulsation was observed in these gain-coupled DFB lasers.

References

- [1] J. Buss, *Electron. Letters* 21 (1985) 179.
- [2] J. Kinoshita and K. Matsumoto, *IEEE J. Quantum Electron.* QE-25 (1989) 1324.
- [3] H. Soda, Y. Kotaki, H. Sudo, H. Ishikawa, S. Yamakoshi and H. Imai, *IEEE J. Quantum Electron.* QE-23 (1987) 804.
- [4] K. David, G. Morthier, P. Vankwikelberge, R.G. Baets, T. Wolf and B. Borchert, *IEEE J. Quantum Electron.* QE-27 (1991) 1714.
- [5] H. Kogelnik and C.V. Shank, *J. Appl. Phys.* 43 (1972) 2327.
- [6] M. Okai, T. Tsuchiya, K. Uomi, N. Chinone and T. Harada, *IEEE J. Quantum Electron.* QE-27 (1991) 1767.
- [7] Y. Luo, Y. Nakano, K. Tada, T. Inoue, H. Hosomatsu and H. Iwaoka, *IEEE J. Quantum Electron.* QE-27 (1991) 1724.
- [8] Y. Luo, Y. Nakano, T. Tada, T. Inoue, H. Hosomatsu and H. Iwaoka, *Appl. Phys. Letters* 56 (1990) 1620.
- [9] E. Kapon, A. Hardy and A. Katzir, *IEEE J. Quantum Electron.* QE-18 (1982) 66.
- [10] G. Morthier, P. Vankwikelberge, K. David and R. Baets, *IEEE Photon. Technol. Letters* PTL-2 (1990) 170.
- [11] K. David, G. Morthier, P. Vankwikelberge and R. Baets, *Electron. Letters* 26 (1990) 238.
- [12] Y. Nakano, Y. Luo and K. Tada, *Appl. Phys. Letters* 55 (1989) 1606.
- [13] Y. Nakano, Y. Deguchi, K. Ikeda, Y. Luo and K. Tada, *IEEE J. Quantum Electron.* QE-27 (1991) 1732.
- [14] T. Inoue, S. Nakajima, T. Oki, H. Iwaoka, Y. Nakano and K. Tada, 17th European Conf. on Optical Communications, Paris, 1991, post-deadline paper 5.
- [15] B. Borchert, K. David, B. Stegmüller, R. Gessner, M. Beschorner, D. Sacher and G. Franz, *IEEE Photon. Technol. Letters* PTL-3 (1991) 953. During the preparation of our manuscript, this reference appeared in print.
- [16] T.K. Koch, P.J. Corvini, U. Koren and W.T. Tsang, *Electron. Letters* 24 (1988) 822.
- [17] W.T. Tsang, M.C. Wu, T. Tanbun-Ek, R.A. Logan, S.N.G. Chu and A.M. Sergent, *Appl. Phys. Letters* 57 (1990) 2065.
- [18] H. Heinecke, B. Baur, N. Emeis and M. Schier, *J. Crystal Growth* 120 (1992) 140.
- [19] T. Tanbun-Ek, R.A. Logan, S.N.G. Chu, A.M. Sergent and K.W. Wecht, *Appl. Phys. Letters* 57 (1990) 2184.
- [20] W.T. Tsang, F.S. Choa, R.A. Logan, T. Tanbun-Ek and A.M. Sergent, *Appl. Phys. Letters* 59 (1991) 1008.
- [21] W.T. Tsang, F.S. Choa, M.C. Wu, Y.K. Chen, R.A. Logan, T. Tanbun-Ek, S.N.G. Chu, K. Tai, A.M. Sergent and K.W. Wecht, *Appl. Phys. Letters* 59 (1991) 2375.
- [22] A. Takemoto, Y. Ohkura, H. Watanabe, Y. Nakajima, Y. Sakakibara, S. Kakimoto and H. Namizaki, in: *Proc. 12th IEEE Intern. Semiconductor Laser Conf.*, Davos, 1990, p. 64.